Symmetry-Breaking Charge-Transfer Chromophore Interactions Supported by Carbon Nanodots**

Michele Cacioppo[+], Tobias Scharl[+], Luka Đorđević,* Alejandro Cadranel, Francesca Arcudi, Dirk M. Guldi,* and Maurizio Prato*

Abstract: *Carbon dots (CDs) and their derivatives are useful platforms for studying electron-donor/acceptor interactions and dynamics therein. Herein, we couple amorphous CDs with phthalocyanines (Pcs) that act as electron donors with a large extended π-surface and intense absorption across the visible range of the solar spectrum. Investigations of the intercomponent interactions by means of steady-state and pump-probe transient absorption spectroscopy reveal symmetry-breaking charge transfer/separation and recombination dynamics within pairs of phthalocyanines. The CDs facilitate the electronic interactions between the phthalocyanines. Thus, our findings suggest that CDs could be used to support electronic couplings in multichromophoric systems and further increase their applicability in organic electronics, photonics, and artificial photosynthesis.*

Multichromophoric systems play an important role in both organic electronics and photosynthetic light harvesting, with the spatial arrangement of the chromophores governing their electronic communication.[1] For example, in the photosynthetic reaction center of purple bacteria, electron transfer from a bacteriochlorophyll "special pair", surrounded by two branches of protein-bound cofactors, is preceded by a symmetry-breaking charge-transfer (SB-CT) state; this is generally defined as arising from a photoexcited process, where a pair of identical chromophores produces a desymmetrized charge-transfer (CT) state. This ultrafast-formed state governs charge separation in photosystem II.[2] Gathering a comprehensive understanding is vital for designing and preparing efficient organic electronic devices. Molecular materials which are capable of undergoing SB-CT will very likely find applications in fields such as organic photovoltaics,[3] photonics,[4] and artificial photosynthesis.[5]

In recent years, there have been many efforts to study interactions between chromophores in nonbiological molecular assemblies. Most notable are pairs of arenes,[6] perylenes,[7] perylene diimides,[8] boron dipyrromethenes/dipyridylmethenes,[9] and metallodipyrrins,[3,10] to name just a few. In terms of effective interchromophore communication, the spacer between them is one of the most critical variables. For example, zinc porphyrins have been linked through phenylene(s),[11] naphthalene,[11,12] phenanthrene,[12] hexaphenylbenzene,[13] hexa-*peri*-hexabenzocoronene bridges,[14] as well as well-defined nanographene spacers.[15] Recently, porphyrins, which were linked through hexa-*peri*-hexabenzocoronene (HBC) spacers, were shown to interact through the π-surface of the HBC. The most compelling evidence for this is a distinct split of the porphyrin Soret-band absorption.[14a]

In the context of photoactive chromophore assemblies, carbon dots (CDs) have been attracting attention.[16] These small (< 10 nm) carbon-based nanoparticles have been employed, both as electron donor (D) and acceptor (A), in

---

[*] M. Cacioppo,[+] Dr. L. Đorđević, Dr. F. Arcudi, Prof. M. Prato
Department of Chemical and Pharmaceutical Sciences
University of Trieste, and INSTM, unit of Trieste
Via Licio Giorgieri 1, 34127 Trieste (Italy)
E-mail: dordevic.luka@gmail.com
        prato@units.it

T. Scharl,[+] Dr. A. Cadranel, Prof. D. M. Guldi
Department of Chemistry and Pharmacy
Interdisciplinary Center for Molecular Materials
Friedrich-Alexander Universität Erlangen-Nürnberg
Egerlandstrasse 3, 91058 Erlangen (Germany)
E-mail: dirk.guldi@fau.de

Dr. L. Đorđević, Dr. F. Arcudi
Present address: Department of Chemistry
Northwestern University
2145 Sheridan Road, Evanston, IL 60208 (USA)

Dr. L. Đorđević
Present address: Simpson Querrey Institute
Northwestern University
303 E. Superior, Chicago, IL 60611 (USA)

Dr. A. Cadranel
Universidad de Buenos Aires
Facultad de Ciencias Exactas y Naturales
Departamento de Química Inorgánica

Analítica y Química Física
Pabellón 2, Ciudad Universitaria
C1428EHA, Buenos Aires (Argentina)
and
CONICET—Universidad de Buenos Aires
Instituto de Química-Física de Materiales
Medio Ambiente y Energía (INQUIMAE)
Pabellón 2, Ciudad Universitaria
C1428EHA Buenos Aires (Argentina)

Prof. M. Prato
Center for Cooperative Research in Biomaterials (CIC biomaGUNE)
Basque Research and Technology Alliance (BRTA)
Paseo de Miramon 182, 20014, Donostia San Sebastián (Spain)
and
Basque Foundation for Science
Ikerbasque, Bilbao 48013 (Spain)

[+] These authors contributed equally to this work.

electron-donor/acceptor systems based on covalent or non-covalent approaches.[17] Notably our groups have previously investigated amorphous nitrogen-doped CDs (referred to as *a*-N-CDs or nitrogen-doped carbon nanodots, NCNDs), and their electron-transfer interactions with a *meso*-tetraarylporphyrin (H$_2$P).[17a] It was found that the covalent NCND-H$_2$P conjugate, immediately after photoexcitation with visible light, undergoes charge separation to form the one-electron-oxidized form of H$_2$P and the one-electron-reduced form of NCND. We now turn our attention to phthalocyanines (Pcs), well-known electron donors, which possess unique properties such as good thermal and (photo)chemical stabilities, as well as intense absorptions in the visible range.[18] Our interest stems also from some previous reports of Pc blends with different CDs, namely, graphitized carbon dots (discoidal and quasi-spherical in shape).[19] These blends were used to improve the absorption of visible light,[19a] to enhance electron-transfer/transport characteristics in inorganic quantum dots solar cells,[19b] and to enhance the nonlinear optical response of the nanomaterials.[19d] It is important to note that no symmetry-breaking charge transfer (SB-CT)/separation (SB-CS) has been observed in any of the aforementioned CD-based D-A materials.

Herein, we report the preparation of a covalent electron-donor/acceptor conjugate consisting of NCNDs and a zinc phthalocyanine (ZnPc). Notably, we show that, upon absorption of light at $\lambda = 387$ nm, the NCNDs carrying the ZnPcs undergo a SB-CT (ZnPc$^{\delta-}$-ZnPc$^{\delta+}$), which is followed by a SB-CS to afford (ZnPc$^-$-ZnPc$^+$). Similarly, after photoexcitation at $\lambda = 675$ nm, a SB-CS is also observed, which, in this particular case, evolved from a hot-S$_1$ state. Taken in concert, the results show that NCNDs provide a scaffold to spatially arrange ZnPcs and facilitate the electronic communication between two or more of them.

The NCND-ZnPc conjugate (Figure 1) was prepared by a carbodiimide (EDC) mediated coupling of the amino groups of the NCNDs[20] and the carboxyphthalocyanine (ZnPc);[21] the characterizations of the conjugate were in accordance with the literature (see the Materials Section in the Supporting Information). Following the reaction and the removal of DMF, the reaction mixture was purified by size-exclusion chromatography (SEC, Sephadex LH-20 resin in methanol). The first dark blue band, corresponding to the NCND-ZnPc conjugate, was collected, the organic solvent was removed under reduced pressure, and the final blue solid was obtained after freeze-drying an aqueous solution. The successful formation of the NCND-ZnPc conjugate was apparent as soon as it was dissolved in methanol, as it had a noticeable difference in solubility in polar organic solvents compared to the starting carboxyphthalocyanine. Furthermore, from a Kaiser test, which was performed with NCNDs and NCND-ZnPc, we estimated the presence of a lower amount of free amino groups (100 µmol g^{-1}) on the nanoparticle surface, compared to pristine NCNDs (1350 µmol g^{-1}). Additional characterization by FTIR spectrophotometry (KBr) confirmed the formation of the amide bond (Figure S1). Specifically, in the conjugate we observe the absence of the ZnPc carboxylic band at $\tilde{\nu} = 1716$ cm^{-1}, the presence of the ZnPc signature bands in the form of C−H
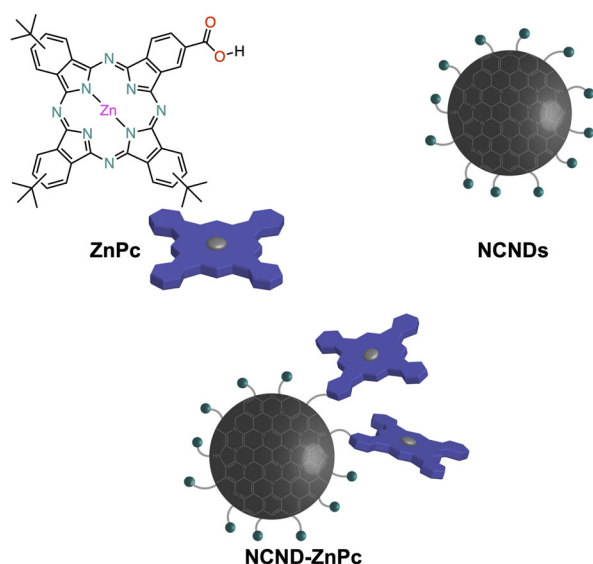

Figure 1. Schematic representation of the ZnPc reference, NCND reference, and NCND-ZnPc conjugate discussed here. NCNDs are represented as an amorphous carbonaceous core (gray) and an amino-rich surface (green color).

stretching at $\tilde{\nu} = 2961$, 2928, and 2850 cm^{-1} as well as C−H bending at $\tilde{\nu} = 1380$ cm^{-1}, and the appearance of C=O and N−H bending signals of amide bands at $\tilde{\nu} = 1637$ and 1565 cm^{-1}, respectively. The composition was further probed by X-ray photoelectron spectroscopy (XPS; Figure S2). The survey spectrum of the hybrid material shows the three peaks corresponding to the C1s, N1s, and O1s species (the atomic percentages for C, N, O are 84.3, 8.0 and 7.7) and the Zn2p$_{3/2}$ species is visible in the high-resolution spectrum. The higher C/N ratio observed for the hybrid (C/N = 10.5) compared to the NCNDs (C/N = 4.25)[20a] is consistent with the presence of the organic macrocycle (deconvoluted spectra are shown in Figure S3). The N1s spectrum also provides evidence of functionalization (Figure S3a,b). It can be deconvoluted into surface components observed for the two single entities,[20a] but the percentage of primary amine is lower compared to the NCNDs alone, in agreement with the decreased value of the Kaiser test.

Thermogravimetric analyses were used to compare the weight residues (or loss) of the hybrid and reference materials (Figure S4). The residual weight at 450°C for the NCND-ZnPc and the NCND alone are 50% and 14%, respectively. Taking into account that zinc phthalocyanines have good thermal stability (>90% residual weight at 450°C),[22] we conclude that the lower residual loss from the conjugate is due to the presence of the ZnPc, and it can be roughly calculated that the latter constitutes about half of the material. Finally, morphological characterization by atomic force microscopy (AFM) showed the presence of larger nanoparticles (4.19 ± 1.11 nm), when compared to pristine NCNDs[20a] (Figure S5).

The optoelectronic properties of the NCND-ZnPc conjugate were first analyzed by comparison with the two references, namely NCNDs and ZnPc, using steady-state absorption and fluorescence spectroscopy (Figure 2, methanol at room temperature).
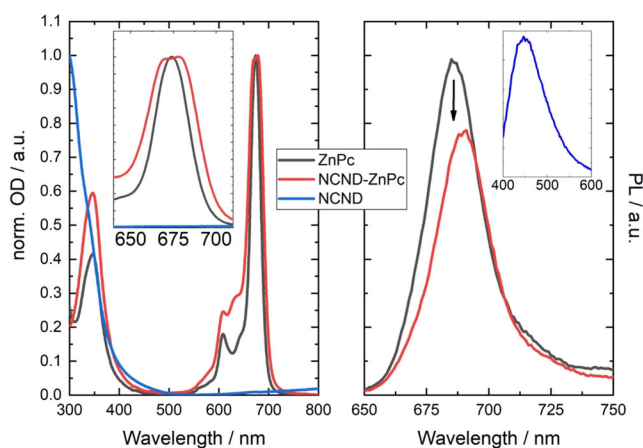
Figure 2. Absorption and fluorescence spectra. Left: Absorption spectra of the NCND reference (blue trace), the ZnPc reference (black trace), and the NCND-ZnPc conjugate (red trace) in methanol at room temperature (the inset shows an enlargement of the Q-band absorption). Right: Fluorescence spectra of the ZnPc reference (black trace) and the NCND-ZnPc conjugate (red trace) with matching absorbance at an excitation wavelength of $\lambda = 387$ nm in methanol and at room temperature (the inset shows the NCND fluorescence upon excitation at $\lambda = 387$ nm in methanol and at room temperature).
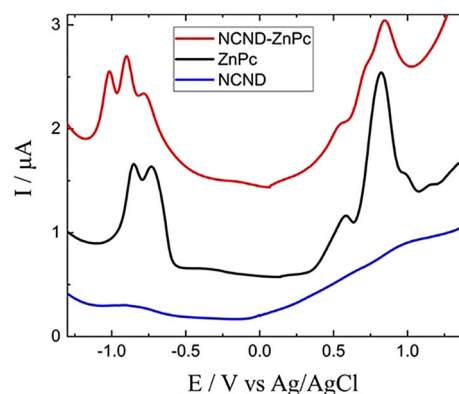

Figure 3. Electrochemistry of the NCND reference (blue trace), ZnPc reference (black trace), and the NCND-ZnPc conjugate (red trace) in methanol at room temperature.

The absorption spectrum of ZnPc shows the typical Q-band absorption at $\lambda = 674$ nm and a weaker Soret-band absorption at $\lambda = 346$ nm. The NCNDs, on the other hand, show the typical absorption spectrum with a broad signal that tails into the visible region. The NCND-ZnPc conjugate presents a different absorption spectrum than the two references. In particular, the Q-band absorptions split into two maxima of similar intensity at $\lambda = 678$ and 670 nm (Figure 2 left, inset). This phenomenon, known as Davydov splitting,[23] is associated with electronic communication between two or more ZnPc units that are in proximity to each other.[14a,24] It is noteworthy that Davydov splitting is not observed in molecular aggregates of ZnPc, since in the latter case a new band appears at $\lambda = 640$ nm (Figure S6). The NCND-ZnPcs were additionally studied in the excited state and, again, compared to the references (Figure 2, right). To excite ZnPc, an excitation wavelength of $\lambda = 387$ nm (3.2 eV) was used and the samples were adjusted to obtain the same optical density. ZnPc shows a strong fluorescence at $\lambda = 686$ nm, with a quantum yield of 0.15. In the NCND-ZnPc conjugate, a fluorescence quenching of 22% is observed, together with a 4 nm red-shift to $\lambda = 690$ nm. An analogous red shift is seen, with a lower fluorescence quenching of 9%, on using an excitation wavelength of $\lambda = 675$ nm (1.84 eV; Figure S7). The difference in the fluorescence quenching efficiency is due to the type of electronic transition which is excited in each particular case (see below). These findings suggest that symmetry-breaking interactions supported by the NCNDs promote additional decay pathways upon excitation.

This aspect was further investigated by electrochemical means (Figure 3). For the NCND reference, rather weak and broad signals, which are hard to dissect, were recorded. The other reference, ZnPc, shows oxidations at $+0.59$ and $+0.82$ V versus Ag/AgCl and reductions at -0.73 and

-0.85 V versus Ag/AgCl. NCND-ZnPc, in contrast, showed three (rather than two) oxidations and reductions at $+0.55$, $+0.72$, $+0.84$ V and -0.78, -0.90, -1.01 V, respectively. This result strongly suggests that, when coupled, the ZnPc-centered orbitals are split because of ground-state electronic interactions with another ZnPc, which is facilitated by the NCNDs. For this reason, a SB-CS state is expected at around 1.33 eV above the ground state.

To better understand the excited-state dynamics responsible for the ZnPc fluorescence quenching, femtosecond time-resolved transient absorption spectroscopy (fsTAS) experiments were performed. These were done for the conjugate and the ZnPc reference, with excitation at $\lambda = 387$ nm in methanol and at room temperature. The ZnPc reference (Figure S8) showed positive transients at $\lambda = 485$, 590, 630, and 808 nm, next to a negative signal at $\lambda = 674$ nm. These features persist to the nanosecond timescale, after which a positive transient at $\lambda = 480$ nm and negative ones at $\lambda = 609$ and 674 nm appear. The global analysis suggests a three-species kinetic model with two exponentially decaying species with time constants of 7 ps and 2.2 ns, together with an infinitely lived species. These two decays are ascribed to an internal conversion $S_1 \leftarrow S_2$ and an intersystem crossing $T_1 \leftarrow S_1$. The triplet (T_1) excited states were much longer-lived with respect to the resolution of the experiments, which in turn helps to rationalize their infinitively lived nature.[25] Similar results were obtained when the ZnPc was excited at $\lambda = 675$ nm (Figure S9). The excitation leads to a hot-S_1 population that decays in 1.6 ps to afford S_1. Then, the intersystem crossing $T_1 \leftarrow S_1$ takes 2.9 ns, preceding the decay to the ground state that occurs on the microsecond timescale.

Compared to ZnPc, NCND-ZnPc shows very different excited state dynamics. Excitation at $\lambda = 387$ nm leads to two minima at $\lambda = 633$ and 670 nm (Figure 4). These signals are accompanied by positive transients at $\lambda = 547$ and 750 nm, which, importantly, were not seen in the ZnPc reference. Moreover, these findings suggest the typical fingerprint absorption of the one-electron-oxidized ZnPc.[26] In contrast, on the nanosecond timescale, the transient absorption spectra resemble those observed for the ZnPc reference. The kinetic model which is derived from these data involves three
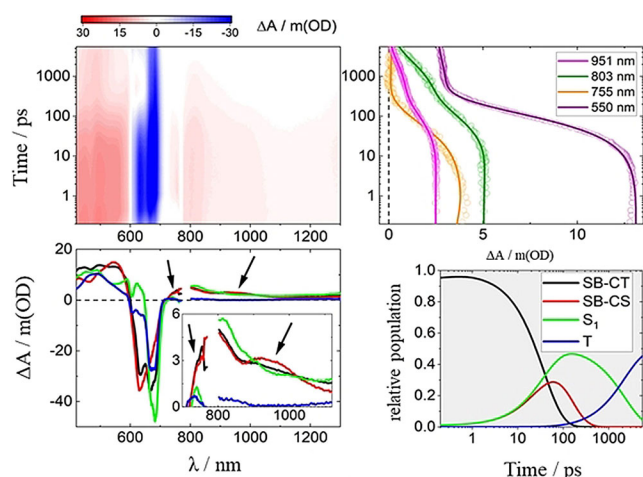
Figure 4. Top left: Differential absorption 3D map obtained upon fsTAS of NCND-ZnPc in methanol at room temperature upon excitation at $\lambda = 387$ nm. Top right: time absorption profiles and corresponding line fittings at $\lambda = 951$ (magenta), 803 (dark green), 755 (orange), and 550 nm (purple). Bottom left: species-associated differential spectra of the SB-CT (black), SB-CS (red), S_1 (green), and T_1 (blue) excited states. Bottom right: concentration evolution over time.

exponentially decaying species and a fourth one, which is persistent on the timescale of these experiments.

Taking also into account the results of fluorescence spectroscopy, a parallel target model was necessary to fit the transient absorption measurements. This model considers two parallel cascades. One of the two cascades, responsible for the fluorescence, includes the same singlet excited state.[27] This intersystem crossing occurs in 2.2 ns to afford the corresponding microsecond-lived triplet excited state that was seen in the ZnPc reference (Figure 5). The second cascade is related to the fluorescence quenching and it is characterized by two excited states with distinct transients at $\lambda = 547$, 750, and 925 nm. Notably, the maxima at $\lambda = 547$ and 750 nm match the ones responsible for the observed formation of one-electron-oxidized ZnPc.[26] The NCNDs in contrast are characterized by a rather broad and featureless band, which extends all across the visible range of the solar
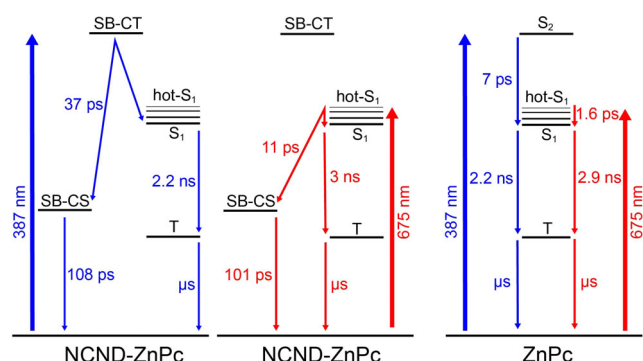
spectrum. Moreover, the one-electron-reduced ZnPc shows a maximum at $\lambda = 1000$ nm[28] that resembles the one recorded for the conjugate. This global information suggests a system formed from a NCND nanoparticle that binds at least two ZnPcs. Here, a SB-CT/SB-CS occurs, by oxidation of one ZnPc moiety, on one hand, and a reduction of another ZnPc moiety, on the other hand. Thus, these two species that are involved in the fluorescence quenching could be assigned in one case to a symmetry-breaking charge-transfer $ZnPc^{\delta-}$-$ZnPc^{\delta+}$ state (SB-CT), which is populated directly upon the absorption of light. In the other case, the cascade could involve the symmetry-breaking charge-separated $ZnPc^-$-$ZnPc^+$ state (SB-CS), which is formed in 37 ps and reinstates the ground state through charge recombination in 108 ps (Figure 5). When excited at $\lambda = 675$ nm, the excited-state dynamics of NCND-ZnPc are quite similar (Figure S10). More specifically, although the SB-CS state evolves from a hot-S_1 state in 11 ps, the charge recombination takes 101 ps, and matches the results obtained on exciting at $\lambda = 387$ nm (Figure 5). To further compare these states, Figure S11 shows the differential spectra of the NCND-ZnPc generated species upon excitation at $\lambda = 387$ and 675 nm.

In summary, we have prepared a covalent conjugate between N-doped carbon nanodots (NCNDs) and zinc phthalocyanines (ZnPcs). Symmetry-breaking (SB) interactions within a ZnPc pair were evident in the absorption profile of the NCND-ZnPc conjugate, which shows the Q-band absorptions presenting Davydov splitting into two maxima of similar intensity. Notably, steady-state fluorescence experiments show quenching in the conjugate, accompanied by a red-shift of the fluorescence maximum, on excitation at both $\lambda = 387$ and 687 nm. This electronic communication, between at least two ZnPc species close to one another on the NCNDs, was confirmed also by electrochemical experiments. Further investigations, by means of steady-state and pump-probe transient absorption spectroscopy, revealed the SB-CT/SB-CS and recombination dynamics in the hybrid material. The present system, therefore, differs from the CND-H$_2$P conjugate, which lacked any evidence of close contacts between the H$_2$Ps on the periphery of the NCNDs.

We have thus provided further evidence of the beneficial integration of CDs into electron-donor/acceptor assemblies, this time by performing a new role as a scaffold. Although precise control of the number and position of the chromophores coupled on the CD surface remains beyond reach, the results presented herein should stimulate further research in CD-based D-A systems and applications in solar-energy conversion. For example, the use of CDs as scaffolds for chromophores of a different nature, as well as using CDs with different structures is envisaged.

Acknowledgements

Figure 5. Target models employed to fit the fsTAS data. Left: NCND-ZnPc conjugate under excitation at $\lambda = 387$ nm. Center: NCND-ZnPc conjugate under excitation at $\lambda = 675$ nm. Right: ZnPc reference under excitation at $\lambda = 387$ and 675 nm.

◤◤ These are not the final page numbers!

Conflict of interest

The authors declare no conflict of interest.

Keywords: carbon dots · charge transfer · chromophores · phthalocyanines · symmetry breaking

[1] a) D. Gust, T. A. Moore, A. L. Moore, *Acc. Chem. Res.* **2001**, *34*, 40–48; b) D. Holten, D. F. Bocian, J. S. Lindsey, *Acc. Chem. Res.* **2002**, *35*, 57–69; c) M. R. Wasielewski, *Acc. Chem. Res.* **2009**, *42*, 1910–1921; d) N. Aratani, D. Kim, A. Osuka, *Acc. Chem. Res.* **2009**, *42*, 1922–1934; e) R. Bhosale, J. Míšek, N. Sakai, S. Matile, *Chem. Soc. Rev.* **2010**, *39*, 138–149; f) F. D'Souza, O. Ito, *Chem. Soc. Rev.* **2012**, *41*, 86–96; g) A. Saeki, Y. Koizumi, T. Aida, S. Seki, *Acc. Chem. Res.* **2012**, *45*, 1193–1202; h) S. Sengupta, F. Würthner, *Acc. Chem. Res.* **2013**, *46*, 2498–2512.

[2] a) S. R. Meech, A. J. Hoff, D. A. Wiersma, *Chem. Phys. Lett.* **1985**, *121*, 287–292; b) D. J. Lockhart, S. G. Boxer, *Biochemistry* **1987**, *26*, 664–668; c) E. J. P. Lathrop, R. A. Friesner, *J. Phys. Chem.* **1994**, *98*, 3056–3066; d) K. N. Ferreira, T. M. Iverson, K. Maghlaoui, J. Barber, S. Iwata, *Science* **2004**, *303*, 1831–1838.

[3] A. N. Bartynski, M. Gruber, S. Das, S. Rangan, S. Mollinger, C. Trinh, S. E. Bradforth, K. Vandewal, A. Salleo, R. A. Bartynski, W. Bruetting, M. E. Thompson, *J. Am. Chem. Soc.* **2015**, *137*, 5397–5405.

[4] E. Collet, M.-H. Lemée-Cailleau, M. Buron-Le Cointe, H. Cailleau, M. Wulff, T. Luty, S.-Y. Koshihara, M. Meyer, L. Toupet, P. Rabiller, S. Techert, *Science* **2003**, *300*, 612–615.

[5] a) B. Rybtchinski, L. E. Sinks, M. R. Wasielewski, *J. Am. Chem. Soc.* **2004**, *126*, 12268–12269; b) A. L. Sisson, N. Sakai, N. Banerji, A. Fürstenberg, E. Vauthey, S. Matile, *Angew. Chem. Int. Ed.* **2008**, *47*, 3727–3729; *Angew. Chem.* **2008**, *120*, 3787–3789.

[6] a) H. Lueck, M. W. Windsor, W. Rettig, *J. Phys. Chem.* **1990**, *94*, 4550–4559; b) F. C. Grozema, M. Swart, R. W. J. Zijlstra, J. J. Piet, L. D. A. Siebbeles, P. T. van Duijnen, *J. Am. Chem. Soc.* **2005**, *127*, 11019–11028.

[7] a) V. Markovic, D. Villamaina, I. Barabanov, L. M. Lawson Daku, E. Vauthey, *Angew. Chem. Int. Ed.* **2011**, *50*, 7596–7598; *Angew. Chem.* **2011**, *123*, 7738–7740; b) A. Aster, G. Licari, F. Zinna, E. Brun, T. Kumpulainen, E. Tajkhorshid, J. Lacour, E. Vauthey, *Chem. Sci.* **2019**, *10*, 10629–10639.

[8] a) M. W. Holman, P. Yan, D. M. Adams, S. Westenhoff, C. Silva, *J. Phys. Chem. A* **2005**, *109*, 8548–8552; b) Y. Wu, R. M. Young, M. Frasconi, S. T. Schneebeli, P. Spenst, D. M. Gardner, K. E. Brown, F. Würthner, J. F. Stoddart, M. R. Wasielewski, *J. Am. Chem. Soc.* **2015**, *137*, 13236–13239; c) J. Sung, A. Nowak-Krol, F. Schlosser, B. Fimmel, W. Kim, D. Kim, F. Wurthner, *J. Am. Chem. Soc.* **2016**, *138*, 9029–9032.

[9] a) M. T. Whited, N. M. Patel, S. T. Roberts, K. Allen, P. I. Djurovich, S. E. Bradforth, M. E. Thompson, *Chem. Commun.* **2012**, *48*, 284–286; b) J. H. Golden, L. Estergreen, T. Porter, A. C. Tadle, D. M. R. Sylvinson, J. W. Facendola, C. P. Kubiak, S. E. Bradforth, M. E. Thompson, *ACS Appl. Energy Mater.* **2018**, *1*, 1083–1095.

[10] C. Trinh, K. Kirlikovali, S. Das, M. E. Ener, H. B. Gray, P. Djurovich, S. E. Bradforth, M. E. Thompson, *J. Phys. Chem. C* **2014**, *118*, 21834–21845.

[11] S. Cho, M. C. Yoon, C. H. Kim, N. Aratani, G. Mori, T. Joo, A. Osuka, D. Kim, *J. Phys. Chem. C* **2007**, *111*, 14881–14888.

[12] N. Toyama, M. Asano-Someda, T. Ichino, Y. Kaizu, *J. Phys. Chem. A* **2000**, *104*, 4857–4865.

[13] a) M. Takase, R. Ismael, R. Murakami, M. Ikeda, D. Kim, H. Shinmori, H. Furuta, A. Osuka, *Tetrahedron Lett.* **2002**, *43*, 5157–5159; b) H. S. Cho, H. Rhee, J. K. Song, C.-K. Min, M. Takase, N. Aratani, S. Cho, A. Osuka, T. Joo, D. Kim, *J. Am. Chem. Soc.* **2003**, *125*, 5849–5860; c) M. M. Martin, M. Dill, J. Langer, N. Jux, *J. Org. Chem.* **2019**, *84*, 1489–1499.

[14] a) M. M. Martin, D. Lungerich, P. Haines, F. Hampel, N. Jux, *Angew. Chem. Int. Ed.* **2019**, *58*, 8932–8937; *Angew. Chem.* **2019**, *131*, 9027–9032; b) M. M. Martin, D. Lungerich, F. Hampel, J. Langer, T. K. Ronson, N. Jux, *Chem. Eur. J.* **2019**, *25*, 15083–15090.

[15] T. Umeyama, T. Hanaoka, H. Yamada, Y. Namura, S. Mizuno, T. Ohara, J. Baek, J. Park, Y. Takano, K. Stranius, N. V. Tkachenko, H. Imahori, *Chem. Sci.* **2019**, *10*, 6642–6650.

[16] a) F. Arcudi, L. Đorđević, M. Prato, *Acc. Chem. Res.* **2019**, *52*, 2070–2079; b) A. Cadranel, J. T. Margraf, V. Strauss, T. Clark, D. M. Guldi, *Acc. Chem. Res.* **2019**, *52*, 955–963; c) Z. Kang, S.-T. Lee, *Nanoscale* **2019**, *11*, 19214–19224; d) C. Xia, S. Zhu, T. Feng, M. Yang, B. Yang, *Adv. Sci.* **2019**, *6*, 1901316.

[17] a) F. Arcudi, V. Strauss, L. Đorđević, A. Cadranel, D. M. Guldi, M. Prato, *Angew. Chem. Int. Ed.* **2017**, *56*, 12097–12101; *Angew. Chem.* **2017**, *129*, 12265–12269; b) K. H. Koh, S. H. Noh, T.-H. Kim, W. J. Lee, S.-C. Yi, T. H. Han, *RSC Adv.* **2017**, *7*, 26113–26119; c) A. Ferrer-Ruiz, T. Scharl, P. Haines, L. Rodríguez-Pérez, A. Cadranel, M. Á. Herranz, D. M. Guldi, N. Martín, *Angew. Chem. Int. Ed.* **2018**, *57*, 1001–1005; *Angew. Chem.* **2018**, *130*, 1013–1017; d) T. Scharl, A. Cadranel, P. Haines, V. Strauss, S. Bernhardt, S. Vela, C. Atienza, F. Gröhn, N. Martín, D. M. Guldi, *Chem. Commun.* **2018**, *54*, 11642–11644; e) A. Cadranel, V. Strauss, J. T. Margraf, K. A. Winterfeld, C. Vogl, L. Đorđević, F. Arcudi, H. Hoelzel, N. Jux, M. Prato, D. M. Guldi, *J. Am. Chem. Soc.* **2018**, *140*, 904–907; f) L. Vallan, R. Canton-Vitoria, H. B. Gobeze, Y. Jang, R. Arenal, A. M. Benito, W. K. Maser, F. D'Souza, N. Tagmatarchis, *J. Am. Chem. Soc.* **2018**, *140*, 13488–13496; g) L. Đorđević, F. Arcudi, A. D'Urso, M. Cacioppo, N. Micali, T. Bürgi, R. Purrello, M. Prato, *Nat. Commun.* **2018**, *9*, 3442; h) T. Scharl, A. Ferrer-Ruiz, A. Saura-Sanmartín, L. Rodríguez-Pérez, M. Ángeles Herranz, N. Martín, D. M. Guldi, *Chem. Commun.* **2019**, *55*, 3223–3226; i) I. Srivastava, J. S. Khamo, S. Pandit, P. Fathi, X. Huang, A. Cao, R. T. Haasch, S. Nie, K. Zhang, D. Pan, *Adv. Funct. Mater.* **2019**, *29*, 1902466.

[18] a) *Phthalocyanines, Properties and Applications* (Eds.: C. C. Leznoff, A. B. P. Lever), VCH, Weinheim, **1993**; b) *Phthalocyanine Materials: Synthesis, Structure and Function* (Ed.: N. B. McKeown), Cambridge University Press, Cambridge, **1998**; c) T. Inabe, H. Tajima, *Chem. Rev.* **2004**, *104*, 5503–5534; d) G. de la Torre, C. G. Claessens, T. Torres, *Chem. Commun.* **2007**, 2000–2015; e) G. de la Torre, G. Bottari, M. Sekita, A. Hausmann, D. M. Guldi, T. Torres, *Chem. Soc. Rev.* **2013**, *42*, 8049–8105; f) L. Martín-Gomis, F. Fernández-Lázaro, Á. Sastre-Santos, *J. Mater. Chem. A* **2014**, *2*, 15672–15682; g) G. Bottari, G. de la Torre, T. Torres, *Acc. Chem. Res.* **2015**, *48*, 900–910.

[19] a) S. Hu, R. Tian, Y. Dong, J. Yang, J. Liu, S. Cao, *RSC Adv.* **2013**, *3*, 21447–21452; b) R. Narayanan, M. Deepa, A. K. Srivastava, *J. Mater. Chem. A* **2013**, *1*, 3907–3918; c) M. K. Barman, B. Jana, S. Bhattacharyya, A. Patra, *J. Phys. Chem. C* **2014**, *118*, 20034–20041; d) N. Nwaji, O. J. Achadu, T. Nyokong, *New J. Chem.* **2018**, *42*, 6040–6050.

[20] a) F. Arcudi, L. Đorđević, M. Prato, *Angew. Chem. Int. Ed.* **2016**, *55*, 2107–2112; *Angew. Chem.* **2016**, *128*, 2147–2152; b) L. Đorđević, F. Arcudi, M. Prato, *Nat. Protoc.* **2019**, *14*, 2931–2953.

[21] J.-J. Cid, J.-H. Yum, S.-R. Jang, M. K. Nazeeruddin, E. Martínez-Ferrero, E. Palomares, J. Ko, M. Grätzel, T. Torres, *Angew. Chem. Int. Ed.* **2007**, *46*, 8358–8362; *Angew. Chem.* **2007**, *119*, 8510–8514.

[22] N. He, Y. Chen, J. Bai, J. Wang, W. J. Blau, J. Zhu, *J. Phys. Chem. C* **2009**, *113*, 13029–13035.

[23] A. S. Davydov, *Sov. Phys. Usp.* **1964**, *7*, 145–178.

[24] J. J. Pie, P. N. Taylor, B. R. Wegewijs, H. L. Anderson, A. Osuka, J. M. Warman, *J. Phys. Chem. B* **2001**, *105*, 97–104.

[25] L. Wibmer, L. M. O. Lourenço, A. Roth, G. Katsukis, M. G. P. M. S. Neves, J. A. S. Cavaleiro, J. P. C. Tomé, T. Torres, D. M. Guldi, *Nanoscale* **2015**, *7*, 5674–5682.

[26] *Handbook of Porphyrin Science, Vol. 9* (Eds.: K. M. Kadish, K. M. Smith, R. Guilard), World Scientific, Singapore, **2010**.

[27] Please note that the fluorescence of S_1 in the nanoconjugate differs somewhat from that of just ZnPc. In turn, the relative population considered for S_1 in NCND-ZnPc might not exactly reflect the 22% fluorescence quenching.

[28] a) P. C. Minor, M. Gouterman, A. B. P. Lever, *Inorg. Chem.* **1985**, *24*, 1894–1900; b) D. W. Clack, J. R. Yandle, *Inorg. Chem.* **1972**, *11*, 1738–1742.
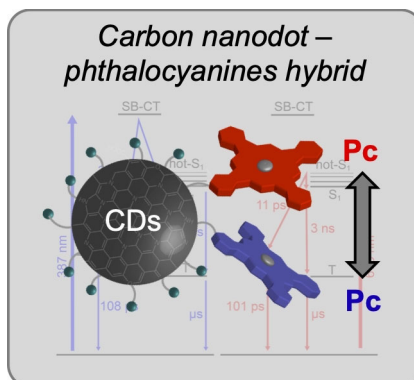
Zuschriften

Charge Transfer

M. Cacioppo, T. Scharl, L. Đorđević,*
A. Cadranel, F. Arcudi, D. M. Guldi,*
M. Prato* ⬛⬛⬛⬛–⬛⬛⬛⬛

Symmetry-Breaking Charge-Transfer
Chromophore Interactions Supported by
Carbon Nanodots

Carbon nanodot – phthalocyanines hybrid

Close encounters: Carbon nanodots have been functionalized with phthalocyanine chromophores by a covalent synthetic approach. This approach made possible the formation of symmetry-breaking charge transfer/separation states between two or more chromophore units connected on the carbon dot surface.